Journal of Biomedical Optics 8(3), 545–551 (July 2003)

Subsurface skin renewal by treatment with a 1450-nm laser in combination with dynamic cooling

Dilip Y. Paithankar
Joan M. Clifford
Bilal A. Saleh
Candela Corporation
530 Boston Post Road
Wayland, Massachusetts 01778
E-mail: dilip.paithankar@clzr1.com

E. Victor Ross
Christina A. Hardaway
David Barnette
Naval Medical Center, San Diego
34520 Bob Wilson Drive
San Diego, California 92134

Abstract. A new nonablative laser device, Smoothbeam, has been under evaluation for nonablative wrinkle reduction in skin with minimal side effects. This device incorporates a laser at 1450-nm wavelength to heat the dermis and cryogen spray cooling to prevent epidermal damage. The thermal injury created is internal and imperceptible. The wound-healing response to this internal injury causes improvement in the appearance of skin wrinkles. Biopsies taken immediately after treatment showed mild residual thermal damage (RTD) at a depth range of 150 to 400 μm, which is the dermal zone where most solar elastosis resides. Biopsies from two months after treatment showed fibroplasia extending over a range of depths similar to the acute RTD zones. An improvement in wrinkle severity was noted on the treated side compared with the control side. [DOI: 10.1117/1.1586703]

Keywords: nonablative wrinkle treatment; cryogen cooling; Monte Carlo light transport modeling.

Paper 01085 received Dec. 19, 2001; revised manuscript received Feb. 25, 2003; accepted for publication Mar. 3, 2003.

1 Introduction

In photodamaged skin, ultraviolet radiation induces solar elastosis, which is the deposition of abnormal yellow amorphous elastotic material that replaces normal collagen and elastin and lacks the resiliency of normal elastic tissue.[1] Also, the superficial collagen fibers appear disorganized when they are examined microscopically. The dermal elastic hypertrophy and disorganized collagen fibers contribute to wrinkles on the face. Wrinkles have been successfully treated by dermabrasion,[2,3] chemical peels,[4,5] and more recently by laser skin resurfacing.[4,6,7] These methods, in general, create a thermal injury within the skin and specifically, lasers allow the clinician to create a controlled thermal injury. The wound-healing response to thermal injury induces production of new collagen in the region of heat-altered dermis, resulting in wrinkle reduction and rejuvenation of skin.[8]

In traditional resurfacing methods, the epidermis and the superficial dermal layers are removed and/or heated. Epidermal destruction implies an open skin wound. The subsequent loss of barrier function results in discomfort as well as dessication-induced extension of the thermal wound.[9–11] Possible complications include persistent erythema, scarring, infection, hyperpigmentation, and hypopigmentation. Furthermore, during the initial healing process, patients experience pain, wound discharge, and swelling. Since the microscopic changes associated with wrinkles occur primarily in the dermis, epidermal removal may be unnecessary for improvement of facial wrinkles.[12,13] Such subsurface skin renewal can be achieved by inducing a subepidermal thermal injury by combining (1) a laser that penetrates deeper than traditional CO_2 or erbium:yttrium aluminum garnet (Er:YAG) resurfacing lasers and (2) cooling of the epidermis. The cooling preserves the epidermis while the laser light heats and insults the dermal collagen. The wound-healing response leads to increased fibroplasia over the period of a few months. Such nonablative subsurface wrinkle removal has been performed with laser light using wavelengths of 1450 nm,[14–17] 1540 nm,[18,19] and 1320 nm.[20,21] These wavelengths employ water as the principal target within skin and cause heating of the dermal collagen. Other nonablative methods targeting the vasculature with wavelengths of 980 nm[22] and 585 nm[23,24] have also been reported. The hypothesized mechanism for treatment with 585-nm light is the heating of blood in the microvasculature, which leads to release of mediators that trigger enhanced collagen production. We present detailed analysis of the method of creating a selective subepidermal thermal injury in the upper portion of the dermis with a 1450-nm wavelength light. The clinical results of wrinkle treatment are also presented.

2 Materials and Mehods

2.1 *Choice of Wavelength*

A review of histology of CO_2 laser-treated skin at three months after treatment indicates that the new organized collagen band extends to about 150 to 400 μm subjacent to the epidermis.[25] Hence, the desired penetration depth of light in skin is about 400 μm. As discussed in the introduction, many wavelengths have been used for nonablative treatments. Most have light penetration depths deeper than 400 μm. For instance, Ross et al.[18] have reported that the heating effect caused by a 1540-nm laser light is deeper than 400 μm. Let us look at the appropriate wavelength for the desired penetration depth. Figure 1 shows a plot of the absorption coefficient of water plotted versus wavelength. The absorption coefficient of water is reported as 28.6 cm^{-1} at a 1450-nm wavelength.[26] If skin is considered to be 70% water, from these proportions the absorption coefficient of skin is estimated to be approximately

1083-3668/2003/$15.00

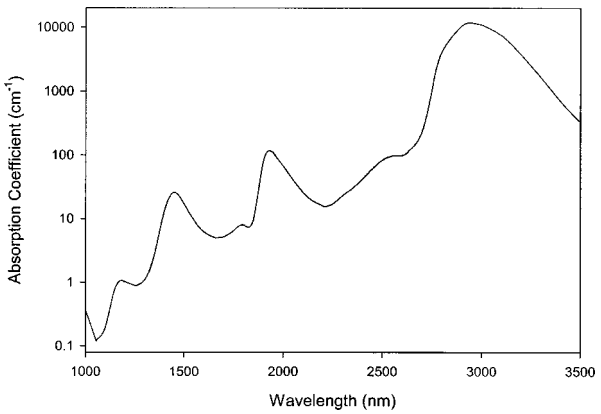

Fig. 1 A plot of the absorption coefficient of water versus wavelength.[9]

$20\ cm^{-1}$. Ignoring scattering effects, the penetration depth can be estimated as the reciprocal of $20\ cm^{-1}$, which is 500 μm. Scattering effects can be taken into consideration through detailed Monte Carlo simulations, which yield, as discussed later, a penetration depth of 439 μm. The heat transfer calculations show that when skin cooling is incorporated, the treatment induces thermal injury in the 100 to 400-μm zone. It is hypothesized that the 1450-nm wavelength would lead to heating that is limited to the upper dermis, where the zone of photodamage and wrinkles resides, leading to high efficacy and reduction of side effects that might be associated with deeper dermal heating. Thus, this wavelength was chosen to produce the desired zone of thermal injury in the dermis. It is expected that the wound-healing response to this injury would lead to new collagen deposition and a reduction in the appearance of wrinkles.

2.2 *Choice of Cooling*

Cutaneous laser treatments have been combined with various cooling methods that can be classified broadly into cryogen spray cooling and contact cooling. In this nonablative approach with water as the chromophore, cryogen spray cooling may be more attractive, owing to its selectivity in cooling the epidermis while leaving the temperature of the deeper structures unchanged.[27] We have chosen this method of cooling; it involves spraying cold cryogen on the treatment area. The cryogen used is tetrafluoroethane, an Environmental Protection Agency approved refrigerant and a Food and Drug Administration approved propellant with a boiling point of $-26\,°C$ at atmospheric pressure.

2.3 *Treatment Device*

The laser device, called Smoothbeam, combines a 1450-nm diode laser with an integrated cryogen spray cooling device called the dynamic cooling device (DCD). The radiant exposure range is from 8 to 20 J/cm^2 delivered with a total duration of 210 ms that is divided into four pulses of equal durations of 52.5 ms each, interspersed with three spurts of cryogen spray. In addition, there is a prelaser spray and a postlaser spray. All sprays are adjustable for precise durations. The timing diagram is shown in Fig. 2, which shows a prespray duration of 15 ms, three intermediate sprays of 15 ms each, and a postlaser spray of 20-ms duration. The laser light from the device is coupled into an optical fiber. The optics at the end of the fiber produces a top-hat, 4-mm diameter circular beam on the skin.

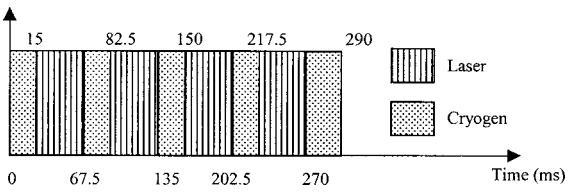

Fig. 2 A timing diagram showing alternate cryogen spray and laser pulses used per treatment shot.

2.4 *Monte Carlo Simulations of Fluence Distribution and Heat Transfer Calculations*

The results of light fluence distribution and temperature and the thermal damage profile are described. These are useful in understanding the temperature distribution and thermal injury for various treatment parameters and for optimization of the same.

In skin, the primary absorber at this wavelength is water and it is assumed that the water content does not vary as a function of depth. Thus, a single-layer model with constant absorption and scattering properties was used. The absorption coefficient (μ_a) of water is dependent on temperature. In the most extreme case, the temperature of the skin upon treatment is expected to increase from about 30 °C to a maximum of 90 °C. The change in the absorption coefficient of water with a 1°C temperature increase has been reported to be $-0.01\ cm^{-1}/°C$ within this range of temperature.[26] For the case of a temperature change of 60 °C, this corresponds to a change in absorption coefficient of $-0.60\ cm^{-1}$. If skin is 70% water, the change in absorption coefficient of skin would be $-0.42\ cm^{-1}$. A change of $0.42\ cm^{-1}$ in the skin absorption coefficient of $20\ cm^{-1}$ is small and hence is neglected. The scattering[20] and absorption properties[26] at a 1450-nm wavelength as given in Table 1 were used as input for the simulations. A homogeneous collimated 4-mm diameter circular beam was incident on the tissue surface.

The tissue volume was discretized into a three-dimensional grid with 41, 41, and 1001 grid points in the x, y, and z directions, respectively, where the z-direction is perpendicular to the skin's surface. The separation between grid points was 0.025, 0.025, and 0.0025 cm in the x, y, and z directions, respectively. Monte Carlo simulations were performed to calculate the light fluence rate, $\phi(x,y,z,t)$, at all grid points

Table 1 Optical properties used in the Monte Carlo model for calculation of light fluence distribution.

Property→ Component↓	Refractive Index (n)	Absorption Coefficient (μ_a)	Scattering Coefficient (μ_s)	Anisotropy Factor (g)
Air	1	0	0	0
Skin	1.37	$20\ cm^{-1}$	$120\ cm^{-1}$	0.9

Table 2 Values of parameters used in the heat transfer calculations.

Laser Fluence	Spot Size	Laser Pulse Duration	Cryogen Temperature	Prelaser Spray Duration	Intermediate Spray Duration (split in 3)	Postlaser Spray Duration	Thermal Diffusivity of Tissue, $\alpha = k/\rho C_p$	Cryogen-skin Heat Transfer Coefficient
16 J/cm^2	4 mm	210 ms	−44°C	15 ms	45 ms	20 ms	8×10^{-4} cm^2/s	4000 W/m^{2}K

within the tissue using the Monte Carlo modeling of light (MCML) software, given the optical absorption and scattering properties of skin.[28,29]

In a second step, heat transfer calculations were performed by solving the heat conduction equation, as given in Eq. (1), numerically by a finite-difference method.

$$\frac{\partial T(x,y,z,t)}{\partial t} = \frac{k}{\rho C_p}\nabla^2 T(x,y,z,t) + \frac{\mu_a \phi(x,y,z,t)}{\rho C_p}, \quad (1)$$

where $T(x,y,z,t)$ is the temperature at location (x,y,z) and time t and k, ρ, and C_p are the thermal conductivity, density, and specific heat of skin, respectively. The last term on the right represents heat generation within tissue that is due to the absorption of light. The boundary condition at the top surface (perpendicular to the z-axis) is described by the convective boundary condition in Eq. (2).

$$-k\frac{\partial T}{\partial z} = h(T_{\text{tissue\_surface}} - T_{\text{coolant}}). \quad (2)$$

In Eq. (2), h is the convective heat transfer coefficient for either the air–skin or cryogen–skin interface. T_{coolant} is the temperature of either cryogen or air that is in contact with the tissue. The air-skin heat transfer coefficient and air temperature are used for the top surface except on the treatment spot, where the respective values for cryogen-skin are used during the time the cryogen spray is incident on the skin. The value of the cryogen-skin heat transfer coefficient has been reported to be as high as 40,000 W/m^2 K[30] and as low as 2400 W/m^2 K.[31] Values of 10,000 W/m^2 K,[32] 6200 to 8400 W/m^2 K,[33] and 5000 W/m^2 K[34] have also been reported. An intermediate value of 4000 W/m^2 K was used in these calculations. A range of values between −37 and −58 °C has been reported for the cryogen temperature. Torres et al.[31] have reported the cryogen temperature to be −44 °C and this value is used. The values of the air-skin heat transfer coefficient and air temperature chosen were 50 W/m^2 K and 30 °C, respectively. The parameters used in the heat transfer calculations are provided in Table 2. In another calculation, no cryogen cooling was incorporated and only the air-skin boundary condition was applied. For the finite-difference heat transfer calculations, the tissue volume was discretized into a three-dimensional grid with 21, 21, and 101 grid points in the x, y, and z directions, respectively. The separation between grid points was 0.05, 0.05, and 0.005 cm in the x, y, and z directions, respectively. The time increment was chosen as 3 ms.

The kinetic thermal damage model relates the temperature-time history of tissue to the thermal damage. The thermal damage measure, Ω, is traditionally defined as the logarithm of the ratio of the original concentration of native tissue, $C(0)$, to the remaining native state tissue, $C(t)$, and by using an Arrhenius-type kinetic model, it is given at a time t by Eq. (3).

$$\Omega(t) = \ln\{C(0)/C(t)\} = \int_0^t \{A\exp(-E_a/RT(\tau)\}\mathrm{d}\tau, \quad (3)$$

where A is a preexponential factor, E_a is the activation energy, R is the universal gas constant, and $T(\tau)$ is the thermal history as a function of time, τ.[35] The parameters A and E_a are typically determined by fitting experimental measurements of damaged and undamaged tissue concentrations as a function of time and temperature. Such thermal damage calculations have been reported previously.[36–38] A representative set of parameters, $A = 1\times10^{75}$ J/mol and $E_a = 5\times10^5$ s^{-1}, has been reported.[35] The damage was calculated as a function of depth in skin through the center of the treated spot by numerically evaluating the integral given in Eq. (3) with the above parameters and the calculated temperature evolution with time.

2.5 *Ex Vivo Histology*

Ex vivo human skin samples obtained from an elective breast reduction were treated with the Smoothbeam. The skin samples were transported at 4 °C and were used in the experiments within 8 h. During the experiment, the skin sample was placed on a metal plate, the temperature of which was maintained at 32 °C by immersing part of it in a temperature-controlled water bath. Treatments were performed on different spots with a 4-mm diameter spot with (1) cryogen spray combined with laser and (2) laser alone. Biopsies were taken with a 3-mm punch and fixed in 10% buffered formalin solution. The samples were processed and stained by hematoxylin and eosin (H&E) stain and examined under an optical microscope.

2.6 *Preliminary Clinical Study*

Two human clinical studies (phases I and II) were conducted. The objective of the phase I clinical study was to evaluate the histological effect of the treatment. Biopsies were performed on skin behind the ear immediately after treatment. The objective of the phase II clinical study was to evaluate the effectiveness of the device for the treatment of periorbital or perioral wrinkles. Nine subjects were enrolled in the phase II clinical study conducted at the Naval Medical Center in San Diego, California. Institutional review board approval was obtained prior to initiation of the study and informed consent was obtained from each of the patients prior to enrollment. The selection of treated and control sides was randomized.

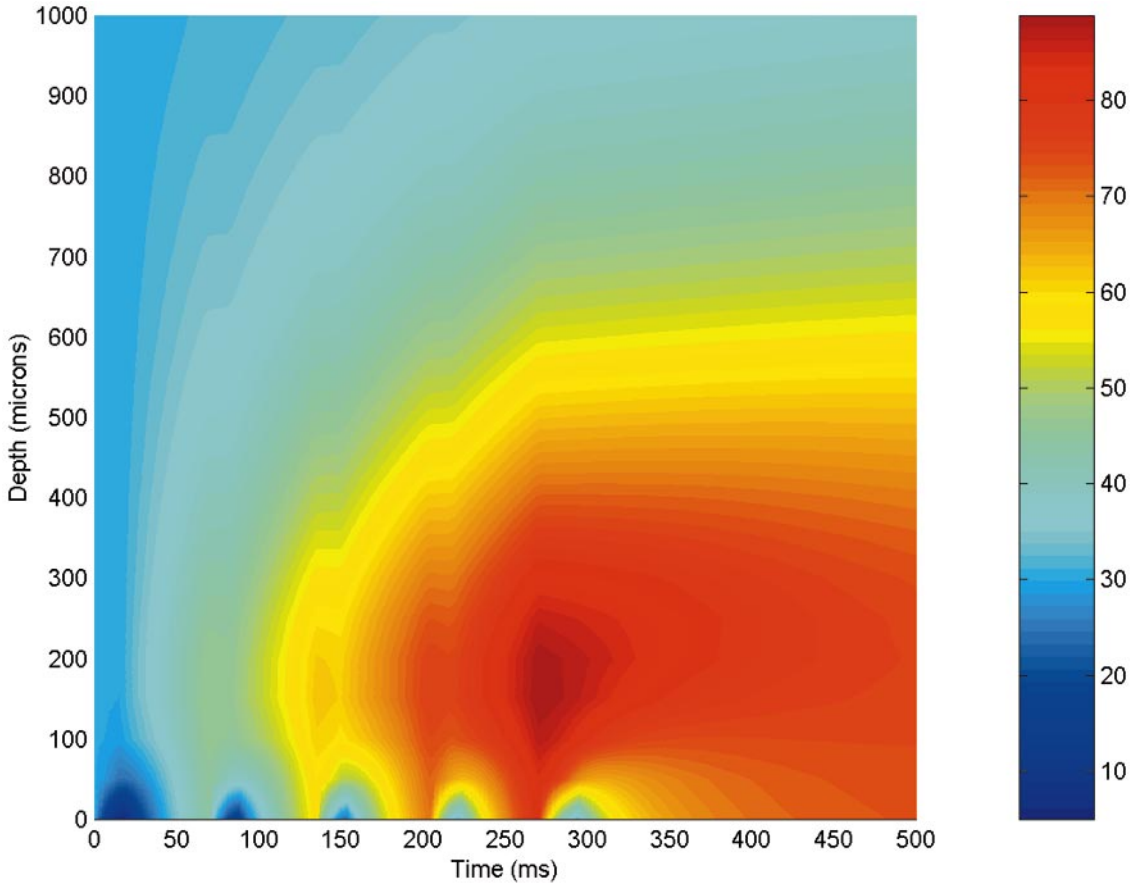

Fig. 3 A plot of temperature versus time and depth. Five cryogen pulses result in epidermal cooling. Thermal heating of the upper dermis is achieved.

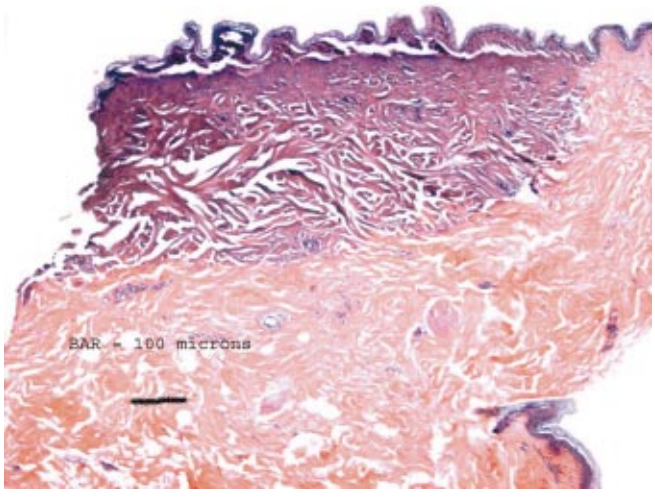

Fig. 6 Histological section of *ex vivo* human skin immediately after treatment with laser alone (H&E). Epidermal separation and thermal damage to the epidermis and upper dermis are seen. On the right, normal skin in the untreated area is seen. Scale bar: 100 μm.

Fig. 7 Histological section of *ex vivo* human skin immediately after laser and DCD treatment (H&E). Epidermal preservation and thermal damage to the upper dermis can be seen. Scale bar: 100 μm.

The treatment area received laser and cryogen, while the control area received only cryogen spray. The timing sequence of the laser and cryogen spray was slightly different than the prior description and the details are given in Refs. 14 and 15. Treatment was given in three rows, a row on top of the wrinkle and two others placed above and below the wrinkle. Three treatments separated by a period of three weeks were administered to the same area. After the first treatment, patients were seen for a one-day and a one-week follow-up. For subsequent treatments, they were seen every three weeks for follow-ups and treatments until each completed a total of three treatments. After the third treatment, patients were seen for follow-up visits at 13 and 23 weeks. Photographs of the treated and control sides were taken before the initial treatment at every treatment or follow-up visit. The radiant exposure was chosen by the clinical investigator so as to be lower than the radiant exposure that caused epidermal whitening. Radiant exposure values ranged between 12.3 and 28.6 J/cm^2. Suggested cooling parameters are 10 ms of prelaser spray, 30 ms of intermediate spray, and 10 ms of postlaser spray.

During all treatments and follow-up visits, the physicians and staff recorded and maintained records of all patients, describing clinical observations associated with the treatments, including wrinkle severity, as well as before and after photographs. The photographs were assessed by observers blinded (unaware) to which side received treatment and which side served as a control. The wrinkle severity was scored on a scale of 1 to 4 as follows: 1, no wrinkling; 2, mild wrinkling; 3, moderate wrinkling; and 4, severe wrinkling. In the data analysis, a comparison of the wrinkle severity score was done to the baseline for both the treated and control sides by performing Student's *t*-test (paired sample).

3 Results

3.1 *Monte Carlo Simulations of Fluence Distribution and Heat Transfer Calculations*

The results of one representative calculation are now discussed. Laser energy of 2.01 J was delivered with the 4-mm circular spot that corresponded to a radiant exposure of 16 J/cm^2. From the calculated results of fluence versus depth through the center of the treatment area, the penetration depth, defined as the depth at which the fluence reaches $(1/e)$, i.e., 36.8% of the fluence at the surface, was evaluated as 439 μm. A cooling scheme that provides a prelaser spray of 15 ms, three intermediate sprays of 15 ms each, and a final postlaser spray of 20 ms was employed. The total laser time of 210 ms was divided into four pulses of equal duration and equal energy. The timing of the heating and cooling pulses is shown in Fig. 2.

Figure 3 shows a plot of temperature versus time and depth. The different colors represent different values of temperature. The epidermis was kept cool by repeated cryogen sprays, and thermal heating of the upper dermis was achieved. The peak temperature was calculated to be 88.8 °C at the end of the last laser pulse at a depth of 150 μm.

Figure 4 shows the damage profile predicted by the kinetic thermal damage model on a log scale as a function of depth along the center of the treatment spot. Thus, the modeling predicts that the combination of DCD cooling and a 1450-nm laser can be used to achieve thermal damage that peaks around a depth of 150 to 200 μm while minimizing the damage in the epidermis and in the deeper dermis. The results predicted through modeling only give qualitative trends and should not be used in inferring quantitative numbers for thermal damage.

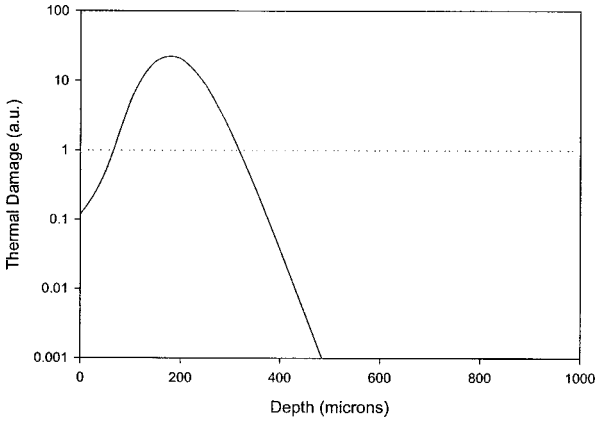

Fig. 4 A plot of thermal damage versus depth with laser and cryogen cooling.

To understand the effect of lasing alone, another heat transfer calculation was performed in which no cryogen cooling was applied. The thermal damage profile versus depth is shown in Fig. 5. As can be seen, thermal damage starts from the top layer of the skin and extends to a depth of about 400 μm from the top.

3.2 *Ex Vivo Histology*

Figure 6 shows a biopsy of an area treated with a fluence of 20 J/cm^2 without any cryogen spray cooling. The photograph shows in the same sample both an untreated area and a treated area. In the treated area, epidermal separation from the dermis is seen. Thermal damage in the dermis is seen and the profile parallels the results of the thermal damage calculations presented in Fig. 5. Figure 7 shows a biopsy for treatment with a radiant exposure of 20.6 J/cm^2, a 10-ms prelaser spray, an intermediate spray consisting of three sprays of 5 ms each, and a postlaser spray of 15 ms. Again, epidermal preservation and selective damage to the upper dermis are seen. This pro-

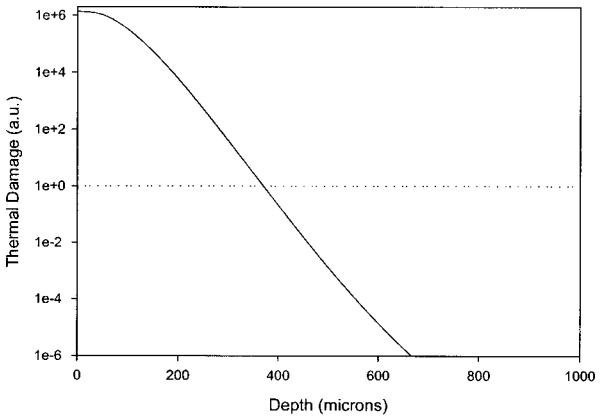

Fig. 5 A plot of thermal damage versus depth after laser treatment without any cryogen cooling.

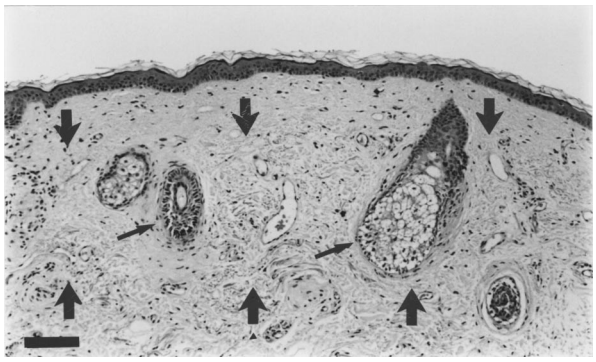

Fig. 8 Immediate post-treatment biopsy demonstrating a band of dermal heat effect (H&E, 40×). The small arrows show elongation of nuclei with thermal damage. The large arrows demarcate superficial and deep boundaries of the heat effect. Scale bar: 100 μm.

vides the proof of principle that epidermal preservation and thermal injury to the upper dermis are indeed possible. The typical laser radiant exposure values used in nonablative treatment of subjects as discussed later are lower than the values used in demonstrating the histology and hence created a milder thermal injury.

3.3 *Preliminary Clinical Study*

In the phase I study, biopsies showed acute mild residual thermal damage (RTD) in the dermis that extended from 150 to 400 μm subjacent to the epidermis, which is the zone where most solar elastosis resides. As seen in Fig. 8, dermal collagen exhibited a zone of slightly basophilic tinctorial changes (the superficial and deep limits of the changes are indicated by the large arrows). The small arrows show elongation of nuclei with thermal damage. Biopsies from two months after treatment showed fibroplasia extending over a range of depths similar to the acute RTD zones as shown in Fig. 9. The arrows demarcate the zone of fibroplasias. In the phase II study, assessment of before and after photographs by a set of blinded observers showed that there was statistically significant wrinkle reduction of 0.35 ($p = 0.007$, < 0.01) on the treated side whereas there was an increase of 0.05 ($p = 0.68$) on the control side. The side effects were limited to erythema and edema that did not exceed two days, while the pain reported was tolerable.

Fig. 9 Two months post-treatment biopsy demonstrating band of dermal fibrosis (H&E, 40×). The arrows demarcate superficial and deep boundaries of fibrosis zone. Scale bar: 100 μm.

4 Conclusions

A new device, Smoothbeam, that combines a diode laser at a 1450-nm wavelength and cryogen cooling has been developed for nonablative treatment of skin wrinkles. The choice of wavelength allows thermal injury in the upper dermis, the principal zone of photoaging. The wound-healing response to the dermal injury allows gradual thermally induced skin renewal. Monte Carlo modeling and heat transfer calculations as well as biopsies and histology of *ex vivo* tissue showed that it is possible to achieve thermal injury in the desired dermal region while preserving the epidermis. In addition, the device was found to be safe and efficacious in the treatment of facial wrinkles in the preliminary human clinical study. The parameters recommended for treatment are a fluence of 14 to 16 J/cm^2 and a DCD setting that includes a 10-ms prelaser spray, three intermediate sprays of 10 ms each, and a postlaser spray of 10 ms.

References

1. J. L. Contenet-Audonneau, C. JeanMaire, and G. Pauly, ''A histological study of human wrinkle structures: comparison between sun-exposed areas of the face, with or without wrinkles, and sun-protected areas,'' *Br. J. Derm.* **140**, 1038–1047 (1999).
2. C. B. Harmon, ''Dermabrasion,'' *Dermatol. Clin.* **19**, 439–442 (2001).
3. G. J. Gruza, ''Dermabrasion,'' *Facial Plast. Surg. Clin. N. Am.* **9**, 267–281 (2001).
4. A. N. Kauvar and J. S. Dover, ''Facial skin rejuvenation: laser resurfacing or chemical peel: choose your weapon,'' *Dermatol. Surg.* **27**, 209–212 (2001).
5. G. D. Monheit, ''Medium-depth chemical peels,'' *Dermatol. Clin.* **19**, 413–425 (2001).
6. R. J. Koch, ''Laser resurfacing of the periorbital region,'' *Facial Plast. Surg.* **15**, 263–270 (1999).
7. R. E. Fitzpatrick, ''CO_2 laser resurfacing,'' *Dermatol. Clin.* **19**, 443–451 (2001).
8. M. P. Goldman and R. E. Fitzpatrick, *Cutaneous Laser Surgery: The Art and Science of Selective Photothermolysis*, 2nd ed., p. 341, Mosby, St. Louis, MO (1999).
9. E. V. Ross, J. R. McKinlay, and R. R. Anderson, ''Why does carbon dioxide resurfacing work?'' *Arch. Dermatol.* **135**, 444–454 (1999).
10. R. E. Fitzpatrick, ''Laser resurfacing of rhytides,'' *Dermatol. Clin.* **15**, 431–447 (1997).
11. M. G. Rubin, ''A peeler's thoughts on skin improvement with chemical peels and laser resurfacing,'' *Clin. Plast. Surg.* **24**, 407–409 (1997).
12. J. M. Stuzin, T. J. Baker, and T. M. Baker, ''CO_2 and Erbium:YAG laser resurfacing: current status and personal perspective,'' *Plast. Reconstr. Surg.* **103**, 588–591 (1999).
13. T. Tsuji, T. Yorifuji, Y. Hayashi, and T. Hamada, ''Two types of wrinkles in aged persons,'' *Arch. Dermatol.* **122**, 22–23 (1986).
14. C. A. Hardaway, E. V. Ross, D. J. Barnette, and D. Y. Paithankar, ''Non-ablative cutaneous remodeling with a 1.45 microm mid-infrared diode laser: phase I,'' *J. Cosmet. Laser Ther.* **4**, 3–8 (2002).
15. C. A. Hardaway, E. V. Ross, and D. Y. Paithankar, ''Non-ablative cutaneous remodeling with a 1.45 microm mid-infrared diode laser: phase II,'' *J. Cosmet. Laser Ther.* **4**, 9–14 (2002).
16. D. J. Goldberg, A. S. Rogachefsky, and S. Silapunt, ''Non-ablative laser treatment of facial rhytides: a comparison of 1450-nm diode laser treatment with dynamic cooling as opposed to treatment with dynamic cooling alone,'' *Lasers Surg. Med.* **30**, 79–81 (2002).
17. E. L. Tanzi, C. M. Williams, and T. S. Alster, ''Treatment of facial rhytides with a nonablative 1,450-nm diode laser: a controlled clinical and histologic study,'' *Dermatol. Surg.* **29**, 124–128 (2003).
18. E. V. Ross, F. P. Sajben, J. Hsia, D. Barnette, C. H. Miller, and J. R.

McKinlay, ''Nonablative skin remodeling: selective dermal heating with a mid-infrared laser and contact cooling combination,'' *Lasers Surg. Med.* **26**, 186 (2000).
19. N. Fournier, S. Dahan, G. Barneon, S. Diridollou, J. M. Lagarde, Y. Gall, and S. Mordon, ''Nonablative remodeling: clinical, histologic, ultrasound imaging, and profilometric evaluation of a 1540 nm Er:glass laser,'' *Dermatol. Surg.* **27**, 799–806 (2001).
20. G. P. Lask, P. K. Lee, M. Seyfzadeh, J. S. Nelson, T. E. Milner, B. Anvari, D. Dave, R. G. Geronemus, L. J. Bernstein, H. Mittelman, L. A. Ridener, W. F. Coulson, B. Sand, J. Baumgarder, D. R. Hennings, R. F. Menefee, and M. Berry, ''Nonablative laser treatment of facial rhytides,'' *Proc. SPIE* **2970**, 338–349 (1997).
21. D. Goldberg, ''Non-ablative subsurface remodeling: clinical and histologic evaluation of a 1320-nm Nd:YAG laser,'' *J. Cutan. Laser Ther.* **1**, 153–157 (1999).
22. J. A. Muccini, F. E. O'Donnell, T. Fuller, and L. Renisch, ''Laser treatment of solar elastosis with epithelial preservation,'' *Lasers Surg. Med.* **23**, 121–127 (1998).
23. B. D. Zelickson, S. L. Kilmer, E. Bernstein, V. A. Chotzen, J. Dock, D. Mehregan, and C. Coles, ''Pulsed dye laser therapy for sun damaged skin,'' *Lasers Surg. Med.* **25**, 229–236 (1999).
24. P. Bjerring, M. Clement, L. Heickendorff, H. Egevist, and M. Kiernan, ''Selective non-ablative wrinkle reduction by laser,'' *J. Cutan. Laser Ther.* **2**, 9–15 (2000).
25. E. V. Ross, Personal Communication, San Diego, CA, July 1, 1999.
26. C. M. Gardner, ''Absorption coefficient of water,'' Personal Communication, In Light Solutions, Albequerque, NM, May 6, 1998.
27. B. Anvari, B. S. Tanenbaum, T. E. Milner, S. Kimel, L. O. Svaasand, and J. S. Nelson, ''A theoretical study of the thermal response of skin to cryogen spray cooling and pulsed laser irradiation: implications for treatment of port wine stain birthmarks,'' *Phys. Med. Biol.* **40**, 1451–1465 (1995) [published erratum appears in *Phys. Med. Biol.* **41**, 1245 (1996)].
28. S. L. Jacques and L.-H. Wang, ''Monte Carlo modeling of light transport in tissue,'' in *Optical Thermal Response of Laser Irradiated Tissue*, A. J. Welch and M. J. C. van Gemert, Eds., Chapter 4, pp. 73–100, Plenum, New York (1995).
29. L.-H. Wang, S. L. Jacques, and L.-Q. Zheng, ''MCML-Monte Carlo modeling of photon transport in multilayered tissues,'' *Comput. Methods Programs Biomed.* **47**, 131 (1995).
30. B. Anvari, T. E. Milner, B. S. Tanenbaum, and J. S. Nelson, ''A comparative study of human skin thermal response to sapphire contact and cryogen spray cooling,'' *IEEE Trans. Biomed. Eng.* **45**, 934–941 (1998).
31. J. H. Torres, J. S. Nelson, B. S. Tanenbaum, T. Milner, D. M. Goodman, and B. Anvari, ''Estimation of internal skin temperatures in response to cryogen spray cooling: implications for laser therapy of port wine stains,'' *IEEE J. Sel. Top. Quantum Electron.* **5**, 1058–1066 (1999).
32. W. Verkruyse, B. Majaron, G. Auilar, L. O. Svaasand, and J. S. Nelson, ''Dynamics of cryogen deposition relative to heat extraction rate during cryogen spray cooling,'' *Proc. SPIE* **3907**, 37–48 (2000).
33. G. Aguilar, B. Majaron, K. Pope, L. O. Svaasand, E. J. Lavernia, and J. S. Nelson, ''Influence of nozzle-to-skin distance in cryogen spray cooling for dermatologic laser surgery,'' *Lasers Surg. Med.* **28**, 113–120 (2001).
34. B. Majaron, G. Aguilar, B. Basinger, L. L. Randeberg, L. O. Svaasand, E. J. Lavernia, and J. S. Nelson, ''Sequential cryogen spraying for heat flux control at the skin surface,'' *Proc. SPIE* **4244**, 74–81 (2001).
35. J. Pearce and S. Thomsen, ''Rate process analysis of thermal damage,'' Chapter 17 in *Optical-Thermal Response of Laser-Irradiated Tissue*, A. J. Welch and M. J. C. van Gemert, Eds., pp. 561–603, Plenum, New York (1995).
36. D. Y. Paithankar, J. Hsia, and E. V. Ross, ''Sub-surface wrinkle removal by laser treatment in combination with dynamic cooling,'' *Proc. SPIE* **3907**, 4–11 (2000).
37. T. J. Pfefer, D. J. Smithies, T. E. Milner, M. J. van Gemert, J. S. Nelson, and A. J. Welch, ''Bioheat transfer analysis of cryogen spray cooling during laser treatment of port wine stains,'' *Lasers Surg. Med.* **26**, 145–157 (2000).
38. G. Aguilar, B. Majaron, J. A. Viator, B. Basinger, E. Karapetian, L. O. Svaasand, E. J. Lavernia, and J. S. Nelson, ''Influence of spraying distance and post-cooling on cryogen spray cooling for dermatologic laser surgery,'' *Proc. SPIE* **4244**, 82–92 (2001).